Available online at www.sciencedirect.com
ScienceDirect
Journal of Environmental Radioactivity 99 (2008) 1143–1148
JOURNAL OF ENVIRONMENTAL RADIOACTIVITY
www.elsevier.com/locate/jenvrad

Estimating the amount and distribution of radon flux density from the soil surface in China

Weihai Zhuo [a,*], Qiuju Guo [b], Bo Chen [a], Guan Cheng [c]

[a] Institute of Radiation Medicine, Fudan University, 2094 Xietu Road, Shanghai 200032, China
[b] Department of Technical Physics, School of Physics, Peking University, Beijing 100871, China
[c] Department of Engineering Physics, Tsinghua University, Beijing 100084, China

Received 27 August 2007; received in revised form 20 January 2008; accepted 21 January 2008
Available online 7 March 2008

Abstract

Based on an idealized model, both the annual and the seasonal radon (^{222}Rn) flux densities from the soil surface at 1099 sites in China were estimated by linking a database of soil ^{226}Ra content and a global ecosystems database. Digital maps of the ^{222}Rn flux density in China were constructed in a spatial resolution of 25 km × 25 km by interpolation among the estimated data. An area-weighted annual average ^{222}Rn flux density from the soil surface across China was estimated to be 29.7 ± 9.4 mBq m^{-2} s^{-1}. Both regional and seasonal variations in the ^{222}Rn flux densities are significant in China. Annual average flux densities in the southeastern and northwestern China are generally higher than those in other regions of China, because of high soil ^{226}Ra content in the southeastern area and high soil aridity in the northwestern one. The seasonal average flux density is generally higher in summer/spring than winter, since relatively higher soil temperature and lower soil water saturation in summer/spring than other seasons are common in China.

Keywords: ^{222}Rn; Flux density; ^{226}Ra content; Ecosystems database; China

1. Introduction

The exhalation of radon (^{222}Rn) from the earth's surface has been studied for many years, and the purposes of studies can be mainly classified into two categories. One is related to the health issue that arises from the public exposure to atmospheric ^{222}Rn and its decay products. Although the indoor environment is more important for the exposure of the public than outdoors, the infiltration of ^{222}Rn from the soil and the building materials made of raw earth have been identified as main factors influencing indoor ^{222}Rn levels in most buildings (Nazaroff et al., 1988; Nielson et al., 1994). Therefore, information on the regional distribution of ^{222}Rn exhalation from the earth's surface is considered as useful for identifying areas with a risk of high radon exposure to public. The other purpose is using ^{222}Rn as a tracer for studying global pollution and climate change, owing to its suitable half-life (3.82 d) and chemically inert (Genthon and Armengaud, 1995; Chino and Yamazawa, 1996). Transfer of ^{222}Rn from soil to the atmosphere involves some of the same processes controlling the soil/air exchange of important greenhouse gases such as CH_4, CO_2 and NO_2. ^{222}Rn does not undergo complicated chemical reactions and its source term is relatively well known (^{226}Ra in soil). Therefore, studies of the ^{222}Rn exhalation are able to provide information on the pure transfer component of gaseous exchange between the soil and the atmosphere.

The ^{222}Rn exhalation rate (flux density) from the ground surface has been used to validate several atmospheric transport computer models in East Asia (Sakashita et al., 1994, 2004; Taguchi et al., 2002). In China, recent surveys have revealed that the nationwide average of indoor ^{222}Rn concentrations has almost doubled over the past 20 years (Shang, 2005). Consequently, exposure to radon has become a public concern in recent years, and it is hoped to create a radon potential map

* Corresponding author. Tel./fax: +86 2164433568.
E-mail address: whzhuo@shmu.edu.cn (W. Zhuo).

0265-931X/$ - see front matter © 2008 Elsevier Ltd. All rights reserved.
doi:10.1016/j.jenvrad.2008.01.011

for China. However, the lack of sufficient data on the distribution of soil ^{222}Rn flux densities across China makes it difficult to create a radon potential map and to accurately validate the regional atmospheric transport computer models.

In this study, an updated model for estimating ^{222}Rn flux densities from the soil surface and a newly constructed database on the soil ^{226}Ra content around China (Zhuo et al., in press) have been linked with the global ecosystems database (GED, Version II) to provide a platform to estimate both the annual and the seasonal ^{222}Rn flux densities from the soil surface across China. The estimated values were further interpolated with a spatial resolution of 25 km × 25 km and edited into digital maps. In addition, the regional and seasonal variations as well as the estimation of uncertainty in the ^{222}Rn flux densities have also been discussed.

2. Methods and data sets

2.1. Model for estimating the ^{222}Rn flux density from the soil surface

The model used in this study had been tested at 20 sites around East Asia (Zhuo et al., 2004, 2006). It is an idealized model for estimating seasonal and annual ^{222}Rn flux densities from semi-infinite and homogeneous soil. The ^{222}Rn flux density (F) from the soil surface was estimated using the following equation,

$$F = A_{\mathrm{Ra}}\rho_{\mathrm{b}}\varepsilon\left(\frac{T}{273}\right)^{0.75}\sqrt{\lambda D_0 p\exp\left(-6Sp-6S^{14p}\right)}, \tag{1}$$

where A_{Ra} is the soil ^{226}Ra content (Bq kg^{-1}), ρ_{b} is the soil bulk density (kg m^{-3}), ε is the emanation coefficient of ^{222}Rn in soil, which is a function of the soil temperature (T, in Kelvin scale) and the water saturation fraction (S), λ is the ^{222}Rn decay constant (s^{-1}), p is the soil porosity, and D_0 is the ^{222}Rn diffusion coefficient in air (1.1×10^{-5} m^2 s^{-1}).

The emanation coefficient (ε) of ^{222}Rn in soil was estimated from the fitted formula of Zhuo et al. (2006),

$$\varepsilon = \varepsilon_0[1 + a(1 - \exp(-bS))]\,[1 + c(T - 298)], \tag{2}$$

where ε_0 is the ^{222}Rn emanation coefficient at a temperature of 298 K for dry soil, and the parameters of ε_0, a, b, and c are taken as constants and are listed in Table 1. The fraction of soil water saturation (S) was estimated using the following function (Zhuo et al., 2006),

$$S = k_0\left(f\frac{E_t}{P}\right)^{-k_1}/p, \tag{3}$$

where (k_0, k_1) = (34.74, 0.3753), (28.49, 0.3748), and (23.39, 0.3773) for soil surfaces covered with forest, grass, and crops, respectively, f is a factor (0.73 for spring, 0.80 for summer, 0.67 for autumn, 0.60 for winter) adjusted for different seasons, E_t is the potential evapotranspiration (mm), and P is the precipitation (mm).

Table 1
Parameters for estimating the ^{222}Rn emanation coefficient in soil

Soil texture[a]	ε_0	a	b	c
Clay	0.10	1.85	18.8	0.012
Silt	0.14	1.73	20.5	0.010
Sand	0.18	1.53	21.8	0.011

[a] Soil texture is classified according to the textural triangle devised by United States Department of Agriculture (USDA).

2.2. Database of soil ^{226}Ra content in China

The database of soil ^{226}Ra content in China used in this study was newly constructed (Zhuo et al., in press). It was spatially interpolated based on the published data from two nationwide surveys (NIRP, 1988; SEPA, 1995). Fig. 1 shows the spatial distribution of soil ^{226}Ra contents with more than 15 000 polygon data in China. The area-weighted average of soil ^{226}Ra content is about 36.6 Bq kg^{-1}, with minima and maxima of 10.5 Bq kg^{-1} and 102.3 Bq kg^{-1}, respectively, for any grid of 25 km × 25 km. In order to minimize the uncertainty brought about by the spatial interpolation, only the 1099 data values without spatial interpolation, which are evenly distributed in a grid of 100 km × 100 km, were used for calculating the ^{222}Rn flux density.

2.3. Ecosystems database

The ecosystems data used in this study include the bulk density, the porosity and texture component (sand, silt, clay) in the top layer (0–30 cm) of the soil, the measured precipitation, the surface temperature, the potential evapotranspiration, and the land cover classification. The resolutions of the ecosystems data are all in grid spacings of 1° × 1° in latitude and longitude. Except for the data set on potential evapotranspiration, which was developed by Ahn and Tateishi (1994), all other data sets are from the global ecosystems database (GED Project, 2000).

2.4. Data readout and digital mapping

All of the necessary ecosystems data were read from the above ecosystems data sets using the spatial coordinates of the soil ^{226}Ra data. After the annual and the seasonal ^{222}Rn flux densities at the 1099 sites in China were calculated, the new soil ^{222}Rn flux density database was edited and imported into an ArcView desktop geographic information system (GIS) of the Environmental Systems Research Institute, Inc. (ESRI). A GIS is a database that links information to location, allowing one to see and analyze data in new and useful ways. The calculated data did not, however, provide enough detail in the ^{222}Rn flux density distribution across China, and so inverse distance weighting (IDW) using the nearest neighbors' mode was used to spatially interpolate the data. This yielded a new polygon database with a spatial resolution of 25 km × 25 km. GIS techniques were then used to create new digital maps of both the annual and the seasonal distributions and provided the data needed for statistical analysis.

3. Results and discussions

3.1. Annual and seasonal ^{222}Rn flux densities from the soil surface in China

Fig. 2 shows the histogram of annual average ^{222}Rn flux densities from the soil surface in China. The data are approximately normally distributed, and the area-weighted annual average ^{222}Rn flux density is 29.7 ± 9.4 mBq m^{-2} s^{-1}, with minima and maxima of 9 mBq m^{-2} s^{-1} and 82 mBq m^{-2} s^{-1}, at a grid scale of 25 km × 25 km, respectively. The ratio of the maximum to the minimum agrees well with the ratio of maximum to minimum soil ^{226}Ra content in the same scale. The area-weighted annual average ^{222}Rn flux density from soil in China is higher than the traditionally assumed average of approximately 21 mBq m^{-2} s^{-1} (1 atom cm^{-2} s^{-1}) for all land surfaces (UNSCEAR, 1982). However, the value is in approximate concordance with the subsequent estimated world average (26 mBq m^{-2} s^{-1}) by UNSCEAR (1993) and also with the latest estimated world average (33 mBq m^{-2} s^{-1}) for dry soil also by UNSCEAR

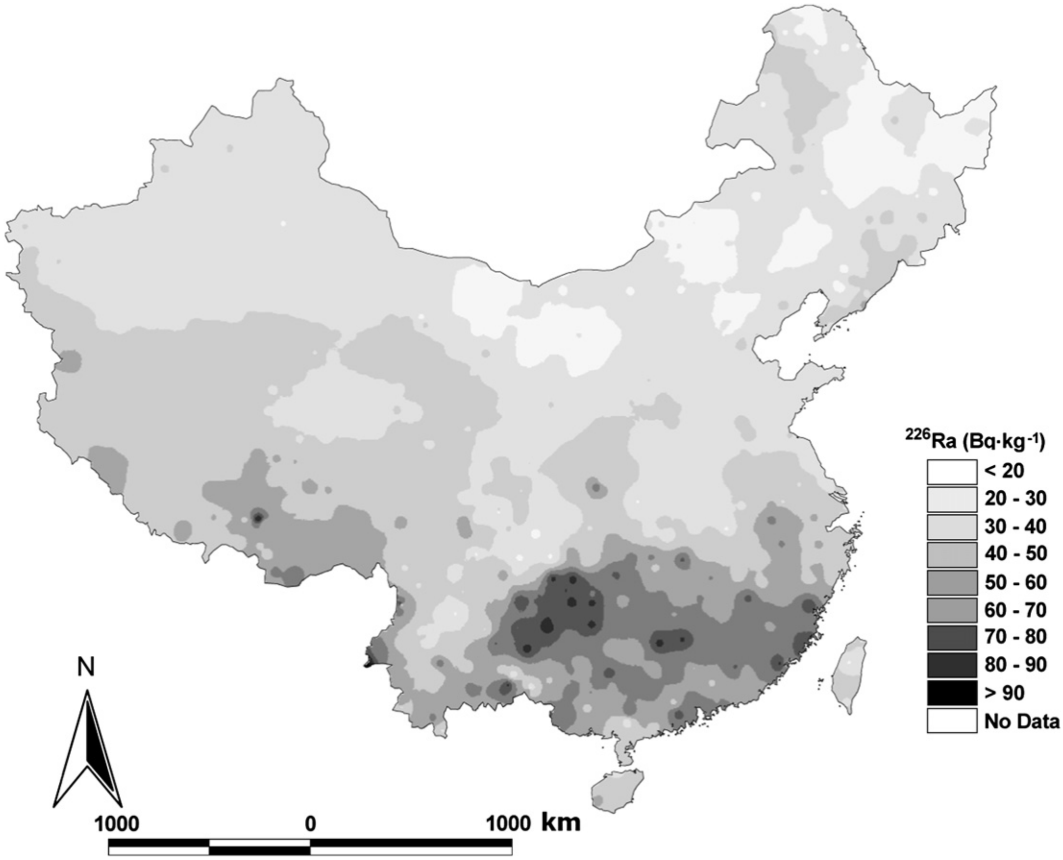

Fig. 1. The distribution of ^{226}Ra contents in surface soil across China.

(2000), as well as with the predicted global average of 34 mBq m^{-2} s^{-1} from ice-free land by Schery and Wasiolek (1998).

Taking the periods of March–May, June–August, September–November, and December–February as spring, summer, autumn and winter, respectively, a box and whisker plot of both the seasonal and the annual ^{222}Rn flux densities from soil surface in China is shown in Fig. 3. The area-weighted averages are 33.1 mBq m^{-2} s^{-1}, 33.6 mBq m^{-2} s^{-1}, 28.9 mBq m^{-2} s^{-1} and 19.2 mBq m^{-2} s^{-1} for spring, summer, autumn and winter, respectively. The averages for both summer and spring are higher than the annual value, while that for winter is much lower.

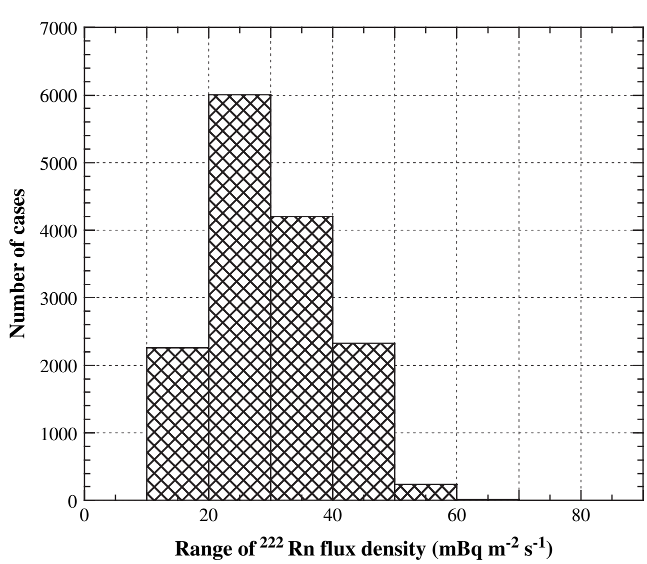

Fig. 2. Histogram of the annual average ^{222}Rn flux density from the soil surface in China.

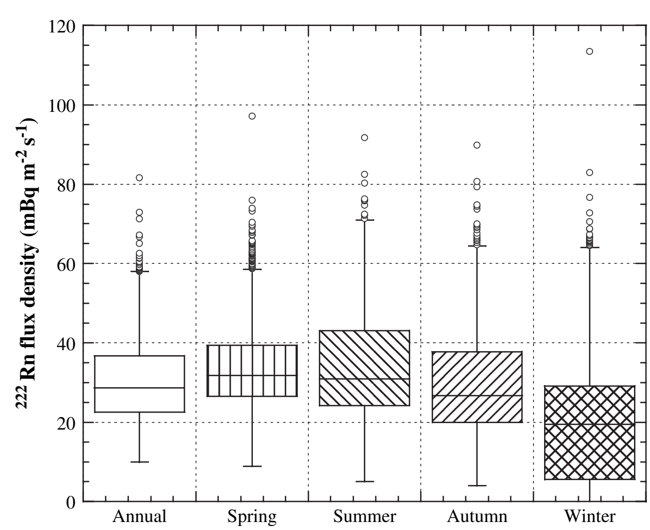

Fig. 3. Box and whisker plot of seasonal and annual ^{222}Rn flux densities from the soil surface in China. Confidence limits (95%) were used for the whisker plot. The open circles are the outliers that lie more than 1.5 times the corresponding lengths of boxes from the upper quartiles.

3.2. Distribution of the annual ^{222}Rn flux density from the soil surface in China

The regional distribution of annual average ^{222}Rn flux densities from the soil surface across China was digitized and mapped and is shown in Fig. 4. The regional variation in the ^{222}Rn flux densities is obvious. The flux density is generally higher in the southeast and northwest regions of China, and generally lower in the northeast and southwest regions. In the southeast region, the higher soil ^{226}Ra content is considered to be the main reason for the higher ^{222}Rn flux density. While in the northwest region, the high soil aridity is thought to bring about the higher ^{222}Rn flux density. In contrast, the lower soil ^{226}Ra content is considered to be the main reason for the lower ^{222}Rn flux density in the northeast region, and the high soil humidity in the Sichuan Basin is expected to be the cause for lower ^{222}Rn flux density in the southwest region.

3.3. Seasonal variations in the ^{222}Rn flux density from the soil surface in China

To assess the seasonal variations in the soil ^{222}Rn flux densities in more detail, we have roughly divided China into six regions, each of which broadly represents a different climatic regime. First, based on the 400 mm isohyet, the line from Mohe (122°22′E, 53°29′N) to Tengchong (98°31′E, 25°01′N) was used as the boundary to separate the east monsoon zone from the west continental zone (Institute of Soil Science, Academia SINICA, 1986). The east monsoon zone was further divided into the south subtropical zone (Lingnan zone, I), north and middle subtropical zone (Huainan and Jiangnan zone, II), south temperate zone (Huabei plain, III), and intermediate temperate zone (Dongbei plain, IV) from the south to the north. The west continental zone was also further divided into the Tibetan plateau (V) and the northwest inland (VI) by using Kunlun Mountains as the boundary. The area-weighted seasonal average ^{222}Rn flux density, temperature and water saturation for the six different climatic zones and for the whole of China are listed in Table 2.

Averaged over the whole country, the ^{222}Rn flux densities in summer and spring are higher than those in other seasons, and the lowest ^{222}Rn flux density occurs in winter. The ratio of the maximum in summer to the minimum in winter is 1.76. It is considered that the higher soil temperature and lower soil water saturation bring out the higher ^{222}Rn flux density in summer, and the lowest soil temperature and higher water saturation cause the lowest ^{222}Rn flux density in winter.

The pattern of seasonal variations in the ^{222}Rn flux density in most of the climate zones is similar to the pattern for the whole country. However, an opposite pattern is found in the Lingnan zone (I), where the maxima and the minima are in winter and summer, respectively. Compared with other zones, the temperature does not change substantially throughout the year, and an opposite seasonal variation in the soil water saturation occurs relative to most of the other zones. In the

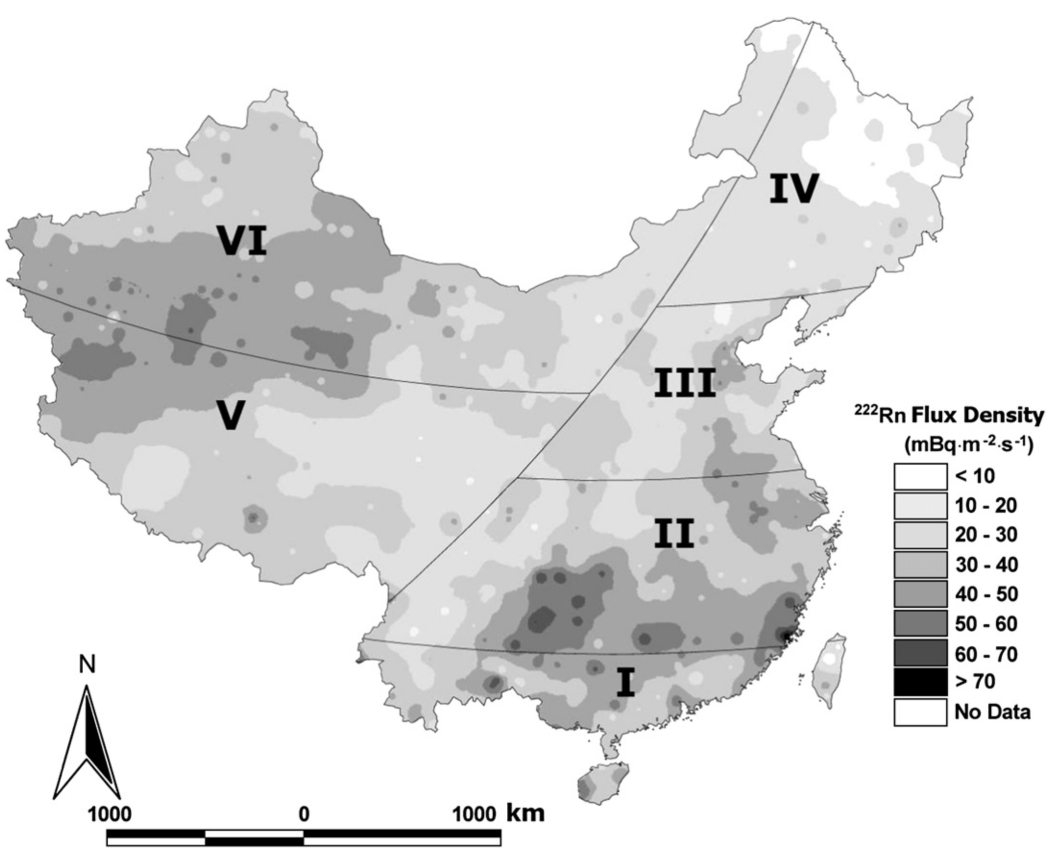

Fig. 4. The distribution of the annual average ^{222}Rn flux density from the soil surface across China.

Table 2
Seasonal average ^{222}Rn flux density (mBq m^{-2} s^{-1}), temperature (in K) and water saturation in the different climatic zones across China

Zone symbol	Item	Spring	Summer	Autumn	Winter	Max/Min
I	Flux	37.0	30.4	37.5	38.9	1.28
	Temperature	294.5	299. 9	295.4	287.4	1.04
	Water saturation	0.57	0.67	0.58	0.51	1.32
II	Flux	33.4	40.4	36.5	27.4	1.47
	Temperature	289.5	298.9	291.0	280.1	1.07
	Water saturation	0.55	0.54	0.55	0.58	1.07
III	Flux	31.5	29.7	25.7	16.4	1.92
	Temperature	285.9	298.3	286.5	271.8	1.10
	Water saturation	0.37	0.49	0.49	0.59	1.64
IV	Flux	22.5	22.2	14.1	0.7	32.1
	Temperature	277.4	293.8	277.7	256.7	1.14
	Water saturation	0.38	0.51	0.61	0.97	2.56
V	Flux	35.7	30.4	28.3	27.0	1.32
	Temperature	282.7	291.0	282.4	272.1	1.07
	Water saturation	0.31	0.47	0.45	0.39	1.52
VI	Flux	34.5	39.0	29.6	10.8	3.61
	Temperature	282.6	295.5	280.7	263.7	1.12
	Water saturation	0.27	0.30	0.37	0.72	2.67
Whole	Flux	33.1	33.6	28.9	19.2	1.76
	Temperature	284.4	295.4	284.2	270.4	1.09
	Water saturation	0.37	0.46	0.48	0.62	1.22

Lingnan zone, the highest seasonal precipitation (752 mm) results in the highest soil water saturation occurring in summer, while the lowest seasonal precipitation (116 mm) causes the lowest soil water saturation in winter. It is noteworthy that the pattern of seasonal variations in the ^{222}Rn flux density in Huainan and Jiangnan zone (II) as well as Lingnan zone (I) is somewhat different from that in other regions. The area-weighted average ^{222}Rn flux density in autumn is slightly higher than that in spring. Analysis shows that the average soil water saturations are nearly the same, however, the average soil temperatures in autumn are slightly higher than those in spring in the two zones. It is consider that the higher seasonal temperature causes the higher ^{222}Rn flux density.

As shown in Table 2, the seasonal variations in the ^{222}Rn flux density in the Dongbei plain (IV) and the northwest inland (VI) are considerably larger than in the other zones. This is attributed to the large variations (>30 °C) in the seasonal soil temperature and the seasonal soil water saturation (>2.5 times) that exist between the summer/spring and the winter seasons. Most of the land in north China is usually covered by snow or the soil is frozen in winter, and it is normally considered that no evapotranspiration occurs. In the present model, ^{222}Rn will not exhale from the soil surface when conditions are such that evapotranspiration is not occurring. However, it has been reported that ^{222}Rn exhalation still occurs from the ground surface during a cold snow season (Yamazawa et al., 2004). This indicates that the model used in this study for predicting ^{222}Rn flux density should be further improved, and that the ^{222}Rn flux density in north China during winter may be underestimated.

3.4. Uncertainty in the estimations

The lack of a sufficient number of measurements of the ^{222}Rn flux density and of the parameters in the ecosystems data set prevents a complete analysis from providing a satisfactory, reliable estimation of the error. However, the uncertainty can be discussed from following viewpoint, and the overall uncertainty is estimated to be roughly ±30% although this is without considering the uncertainty from the ecosystems data.

To verify the model predictions of the ^{222}Rn flux from soil surfaces, field measurements were continuously performed at 20 sites in China, Japan and Korea throughout fiscal year 2003 (Zhuo et al., 2004). The soil ^{226}Ra contents and bulk densities were in the ranges 17.5–115.5 Bq kg^{-1} and 920–1680 kg m^{-3} across the sites, and the annual averaged surface soil temperature and the annual precipitation were in the ranges 5.2–19.7 °C and 350–2330 mm for the sites, respectively. The annual average ^{222}Rn flux density (21.7 mBq m^{-2} s^{-1}) predicted by the model for the 20 sites was only about 10% less than the measured average (24.1 mBq m^{-2} s^{-1}), and deviations of predicted values from measured ones ranged from −22.6% to 17.8% over the sites. To estimate the ^{222}Rn flux densities across the whole of China for this study, the soil ^{226}Ra contents and bulk densities are in the ranges 10.5–102.3 Bq kg^{-1} and 800–1900 kg m^{-3}, and the annual averaged surface soil temperature and annual precipitation are in the ranges −4.5–26.0 °C and 18–2817 mm, respectively, for any grid of 25 km × 25 km grid. The ranges in the soil ^{226}Ra contents and the ecosystems data (bulk density, temperature and precipitation) measured for the 20 sites therefore almost cover the data used in the estimates for the whole of China. Accordingly, provided that the input parameters (A_{Ra}, ρ_b, ε_0, T, E_t and P) were accurate, the estimation uncertainty from the model itself is expected to be about ±20% in any of the 25 km × 25 km grids across the whole of China.

The uncertainties in the soil bulk density (ρ_b), surface soil temperature (T), potential evapotranspiration (E_t) and precipitation (P) from the ecosystems database are unknown, hence only the effect of the uncertainties in the input parameters for the soil ^{226}Ra content (A_{Ra}) and the ^{222}Rn emanation coefficient at 298 K for dry soil (ε_0) are discussed here. A previous study reported that the area-weighted average soil ^{226}Ra contents used in this study were 0.3% higher than the result of a nationwide survey, and the deviation of interpolated data from measured values ranged from −6% to 11% across the 32 provinces, cities and autonomous regions of China (Zhuo et al., in press). The ε_0 values used in this study were from the measurements of 20 soil samples, and the model of ^{222}Rn emanation coefficient was built under the experimental conditions using soil temperatures of −20–45 °C and soil water saturations of 0.01–0.80 (Iskandar et al., 2004; Zhuo et al., 2006). Although the parameter of ε_0 and the emanation model are based on limited experiments, the estimated ^{222}Rn emanation coefficients are in general agreement with other reported values. In this study, the seasonal average ^{222}Rn emanation coefficients were estimated to be in the range 0.14–0.51 for all types of soils, with an annual average of 0.31 for the whole of China. The seasonal ^{222}Rn emanation coefficients in China are in the range of typical ^{222}Rn emanation coefficients (0.05–0.7) for rocks and soils (UNSCEAR, 2000). The annual averaged ^{222}Rn emanation coefficient in China also agrees well with the average of 0.30 for 21 soil samples with unknown moisture content reported by Barreto (1974).

4. Conclusions

Both the annual and the seasonal ^{222}Rn flux densities from the soil surface were estimated for 1099 sites evenly distributed across China, and the data were further interpolated into a spatial resolution of 25 km × 25 km and digitally mapped. The following points can be concluded from the above results and discussions.

(1) The area-weighted annual average ^{222}Rn flux density from the soil surface in China was estimated to be 29.7 ± 9.4 mBq m^{-2} s^{-1}. It is higher than the traditionally assumed world average, but in approximate concordance with the later estimated global average by UNSCEAR.
(2) A significant regional distribution of the ^{222}Rn flux densities from the soil surface exists across China. The annual averages in the southeast and northwest are generally higher than those in other regions of China. The ratio of the maximum to the minimum flux density is about 9 at a grid scale of 25 km × 25 km.
(3) The seasonal variation in the ^{222}Rn flux densities emanating from the soil surface across China is readily apparent and quite complicated. In general, higher ^{222}Rn flux densities exist in summer/spring, while lower values are present in winter. However, the opposite pattern occurs in the south subtropical parts of China. The seasonal variations in the ^{222}Rn flux densities of northern China are considerable (>a factor of 3) owing to large seasonal variations in soil temperature and water saturation.
(4) Without consideration of the errors existing in the ecosystems data, the overall uncertainty for the prediction of the annual average ^{222}Rn flux density in China using a spatial resolution of 25 km × 25 km is estimated to be ±30%. The models for predicting the ^{222}Rn flux density should be further improved in the future. More laboratory measurements of ^{222}Rn emanation coefficients and more field measurements of the ^{222}Rn flux density are needed to further verify the reliability of this estimate.

Acknowledgement

This work was supported by the Ministry of Education, Culture, Sports, Science and Technology, Japan and the National Science Foundation of China (Grant No. 10575023).

References

Ahn, C.H., Tateishi, R., 1994. Development of global land surface evapotranspiration and water balance data sets. Journal of Japan Society of Photogrammetry and Remote Sensing 33, 51–64.

Barreto, P.M.C., 1974. Emanation Characteristics of Terrestrial and Lunar Materials and the Radon-222 Loss Effect on the Uranium–lead System Discordance. Ph.D. dissertation. Rice University, Houston, Texas.

Chino, M., Yamazawa, H., 1996. Development of an atmospheric ^{222}Rn concentration model using a hydrodynamic meteorological model: three-dimensional research-purpose model. Health Physics 70, 55–63.

Genthon, C., Armengaud, A., 1995. Radon-222 as a comparative tracer of transport and mixing in two general circulation models of the atmosphere. Journal of Geophysics Research 100 (D2), 2849–2866.

Global Ecosystems Database Project, 2000. Global Ecosystems Database Version II: Database, User's Guide, and Dataset Documentation. US Department of Commerce, National Oceanic and Atmospheric Administration, National Geophysical Data Center, Boulder, Colorado. KGRD #35. Two CDROMs and publication on the world wide web.

Iskandar, D., Yamazawa, H., Iida, T., 2004. Quantification of the dependency of radon emanation power on soil temperature. Applied Radiation Isotopes 60 (6), 971–973.

Institute of Soil Science, Academia SINICA, 1986. The Soil Atlas of China. Cartographic Publishing House, Beijing (in Chinese).

National Institute for Radiological Protection of China CDC, 1988. Levels and distributions of natural radionuclides in soil in China. Chinese Journal of Radiological Medicine and Protection 8 (Suppl. 2), 1–16 (in Chinese).

Nazaroff, W.W., Moed, B.A., Sextro, R.G., 1988. Soil as a source of indoor radon: generation, migration, and entry. In: Nazaroff, W.W., Nero, A.V. (Eds.), Radon and its Decay Products in Indoor Air. Wiley-Interscience, New York, pp. 57–112.

Nielson, K.K., Rogers, V.C., Holt, R.B., 1994. The RAETRAD model of radon generation and transport from soils into slab-on-grade houses. Health Physics 67, 363–377.

Sakashita, T., Murakami, T., Iida, T., Ikebe, Y., Suzuki, K., Chino, M., 1994. A numerical model of three-dimensional atmospheric transport with application to the transport of ^{222}Rn. Journal of Atmospheric Electricity 14, 57–62.

Sakashita, T., Doi, M., Nakamura, Y., Iida, T., 2004. A case study of radon-222 transport from continental North-East Asia to the Japanese islands in winter by numerical analysis. Journal of Environmental Radioactivity 72, 245–257.

Schery, S.D., Wasiolek, M.A., 1998. Modeling radon flux from the earth's surface. In: Proceedings of Seventh Towa University International Symposium, Fukuoka, Japan, pp. 207–217. ISBN 981-02-3443-0.

State Environmental Protection Administration of China, 1995. Levels of Naturally Environmental Radiation in China. SEPA, Beijing, pp. 167–675 (in Chinese).

Shang, B., 2005. Radioactive pollution and health. In: Xu, D.Q. (Ed.), Air Pollution and Health in Dwelling Environment. Chemical Industry Press, Beijing, pp. 198–251 (in Chinese).

Taguchi, S., Iida, T., Moriizumi, J., 2002. Evaluation of the atmospheric transport model NIRE-CTM-96 by using measured radon-222 concentration. Tellus 54B, 250–268.

United Nations Scientific Committee on the Effects of Atomic Radiation (UNSCEAR), 1982. Ionizing Radiation: Sources and Biological Effects. United Nations, New York, 152 pp.

United Nations Scientific Committee on the Effects of Atomic Radiation (UNSCEAR), 1993. Sources, Effects and Risks of Ionizing Radiation. United Nations, New York, 46 pp.

United Nations Scientific Committee on the Effects of Atomic Radiation (UNSCEAR), 2000. Sources and effects of ionizing radiation, vol. 1. United Nations, New York, pp. 98–99.

Yamazawa, H., Miyazaki, T., Moriizumi, J., Iida, T., Takeda, S., Nagara, S., Sato, K., Tokizawa, T., 2004. Radon exhalation from a ground surface during a cold snow season. Elsevier International Congress Series, vol. 1276, pp. 221–222.

Zhuo, W., Furukawa, M., Guo, Q., Kim, Y.S., 2004. Soil radon flux and outdoor radon concentrations in East Asia. Elsevier International Congress Series, vol. 1276, pp. 285–286.

Zhuo, W., Iida, T., Furukawa, M., 2006. Modeling radon flux density from the earth's surface. Journal of Nuclear Science and Technology 43, 479–482.

Zhuo, W., Chen, B., Li, D., Liu, H. Reconstruction of database on natural radionuclide content in soil in China. Journal of Nuclear Science and Technology 45, in press.